Open Access Online Journal on Astronomy and Astrophysics

Acta Astrophysica Taurica

www.astrophysicatauricum.org

Acta Astrophys. Tau. 3(2), 22–26 (2022)

Characteristics of the radiation of polar coronal holes on the Sun in a wide range of radio waves

O.A. Golubchina

St. Petersburg Branch of the Special Astrophysical Observatory, St. Petersburg 196140, Russia
e-mail: golubchina_olga@mail.ru

Submitted on October 2, 2021

ABSTRACT

The paper presents a brief overview of the main results of observations of the radio emission in polar coronal holes on the Sun obtained in a wide range of wavelengths with various radio telescopes. We analyze the results of observations of the polar coronal hole with RATAN–600 in a wide centimeter wavelength range of (1.03–30.7) cm. The obtained physical characteristics of the coronal hole above the north pole of the Sun are compared with the characteristics of the coronal holes located at lower latitudes.

Key words: Sun, coronal holes, radio emission

1 Introduction

Polar coronal holes (CHs) are always seen at the solar poles within the periods of minimal solar activity since the rotation-oriented dipole magnetic field component predominates at this time. CHs are characterized as the regions of reduced

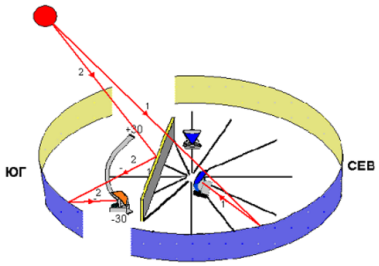

Fig. 1. Layout of the RATAN-600 radio telescope. (1 – an incident beam from the Sun while observing in the north-east sector of RATAN-600; 2 – while observing in the south sector of RATAN-600)

temperature and solar atmosphere density. These are unipolar regions with open magnetic field configuration. In this paper we provide an analysis of the results of observations of the polar coronal hole radio emission during the maximal phase of the solar eclipse on March 29, 2006 in the relay-race mode at the north-east sector of the radio astronomical telescope of the Academy of Sciences (RATAN-600, Fig. 1) at wavelengths of $\lambda = (1.03, 1.38, 2.7, 6.2, 13.0, 30.7)$ cm (Golubchina et al., 2011). At the moment of the maximal phase of the solar eclipse the open part of the optical solar disk was 0.2 % (Fig. 2).

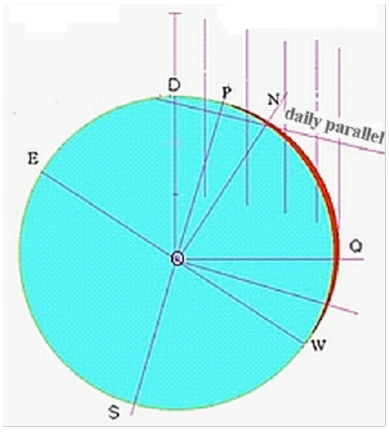

Fig. 2. Position of the knife-edge diagram at different moments of the solar eclipse during the passage of the Sun and the Moon through the antenna pattern of RATAN-600

Table 1. Angular sizes of the horizontal (ρ_h) and vertical (ρ_v) antenna patterns of RATAN-600 at observational wavelengths. Here λ is the wavelength of observations.

λ cm					
1.03	1.38	2.7	6.2	13	30.7
($\rho_h \times \rho_v$) arcmin					
0.4×17.3	0.6×19.3	1.2×19.4	2.6×25.0	5.7×35.8	13.4×84.4

The RATAN-600 radio telescope has a knife-edge antenna pattern (AP) (Table 1).

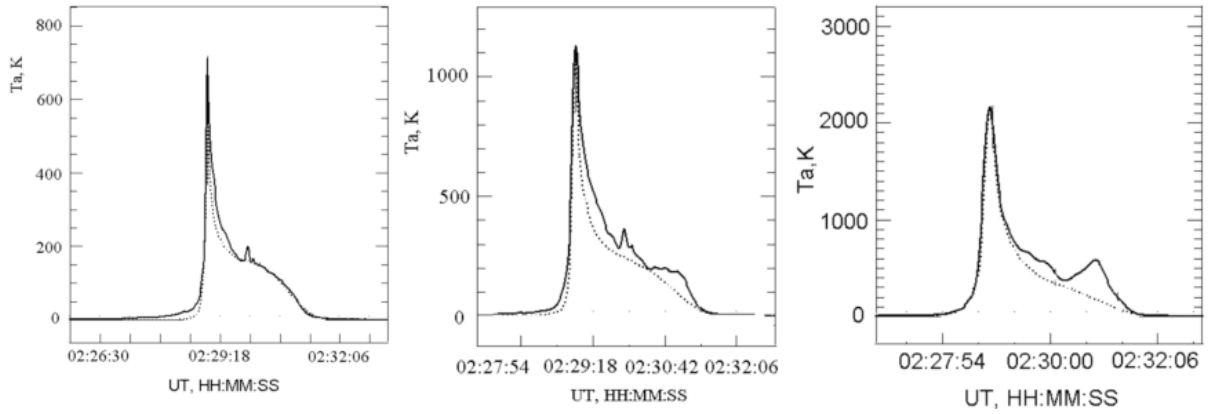

Fig. 3. Model (dashed line) and obtained from eclipse observations (solid line) curves of radio emission from the Sun and the Moon at wavelengths of λ = 1.38 cm (left panel), 2.7 cm (central panel), 6.2 cm (right panel).

2 Observation of the solar eclipse on March 29, 2006 with RATAN-600

The center of the AP while observing the maximal phase of the solar eclipse was shifted to the north pole of the Sun with respect to the center of the solar optical disk at a height of +15 angular minutes (Fig. 2). This allowed us to determine the physical characteristics of the weak emission of the polar CH above the north pole of the Sun (Golubchina et al., 2011).

The aim of observing the solar eclipse on March 29, 2006 with RATAN-600 was a determination of the brightness temperatures from the solar limb up to the distances of 2 Rs from the center of the solar optical disk (Rs is the radius of the solar optical disk). This task was resolved by creating the semi-empirical models of the Sun and the Moon. The brightness temperatures of the Sun (Moon) were specified either according to the literature data (Zheleznyakov, 1964; Sobolev, 1967) or by fitting them using the trial-and-error method, or by the solution of the transfer equation, or by combing all the listed methods (Golubchina et al., 2011). When observing a radio emission source the radio signal is recorded at the antenna temperatures T_a. The antenna temperatures of models are determined by substituting the selected brightness temperatures into equation (1) for the antenna smoothing of brightness temperatures by the antenna pattern:

$$T_a(\varphi_0) = \int T_b(\varphi_0) A(\varphi - \varphi_0) d\varphi, \qquad (1)$$

where $T_b(\varphi_0)$ is the brightness temperature of a radio emission source, $A(\varphi - \varphi_0)$ is the vertical antenna pattern, $\varphi - \varphi_0$ is the angle of deflection from the center of the antenna pattern.

To solve the task, it is required to select brightness temperatures in such a way that at their substituting into equation (1) the obtained antenna temperatures would be as close as possible to the observed ones. The degree of matching the antenna temperatures of the model source with antenna temperatures in the actual record of the observed radio emission source is a quality assessment of the modeling. Figure 3 demonstrates a high degree of matching the actual record (solid line) with the model one (dashed line). This means that the generated model has a good quality. Thus, the selected brightness temperatures which are consistent with the antenna temperatures of an actual observation are the detected distribution of brightness temperatures above the northern region of the Sun where a polar CH is located.

3 Comparison of the obtained model and actual observations

The distribution of brightness temperatures in the region of a polar CH of the Sun was first determined in a wide centimeter wavelength range according to observations of the solar eclipse on March 29, 2006 with the RATAN-600 radio telescope (Fig. 4).

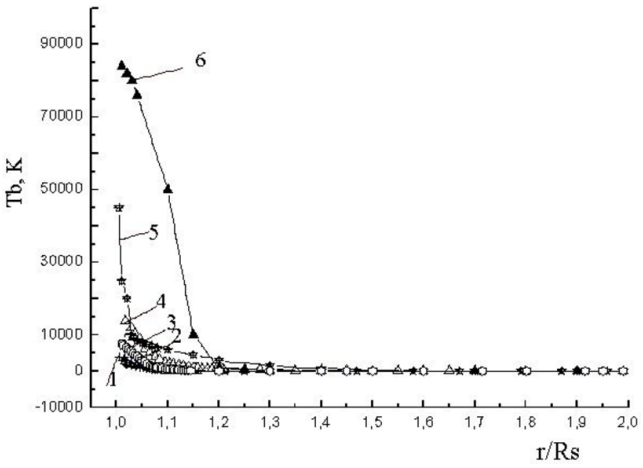

Fig. 4. Distribution of the brightness temperature (Tb) with a distance from the center of the solar optical disk (Rs) in the polar coronal region of the Sun at the following wavelengths: 1 – 1.03 cm; 2 – 1.38 cm, 3 – 2.7 cm, 4 – 6 cm, 5 – 13 cm, 6 – 30.7 cm (Golubchina, 2021).

An abrupt decrease in brightness temperatures of the radio emission from the polar CH was recorded at the radio wavelengths of λ = 13.0 cm at a distance interval from the

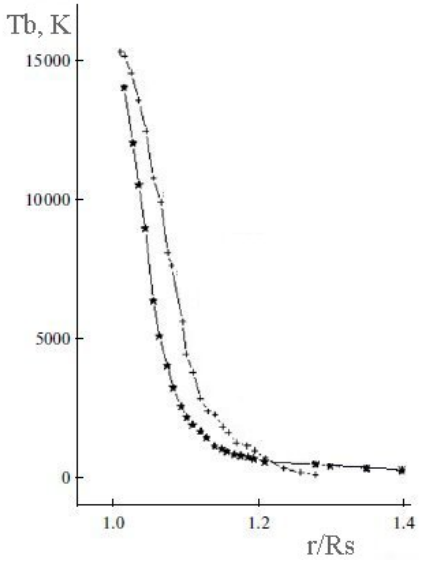

Fig. 5. Brightness temperature distribution in the solar corona at a distance interval of (1–1.4) r/Rs. Here (⋆) denotes the brightness temperature values (Tb, K) of the polar CH which were detected while observing the solar eclipse on March 29, 2006 at $\lambda = 6.2$ cm; (+) denotes the values of (Tb, K) (Borovik, 1994) for the quiet Sun at a close wavelength of 4.0 cm.

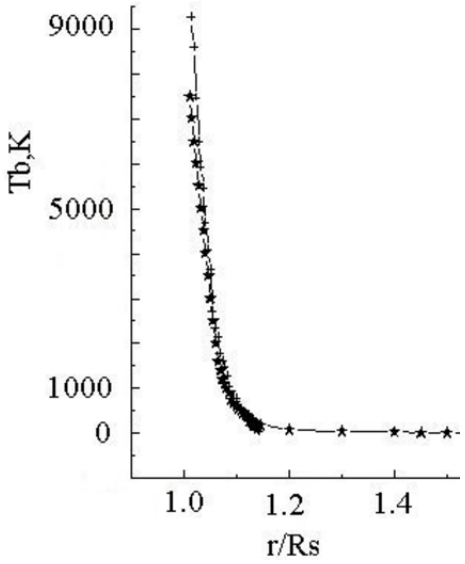

Fig. 6. Brightness temperature distribution of the Sun obtained during the solar eclipse on March 29, 2006 (⋆) and that of the quiet Sun (+) at $\lambda = 2.7$ cm.

solar limb of (1.005–1.03) r/Rs and at the wavelength $\lambda = 30.7$ cm at a distance interval of (1.01–1.15) r/Rs. No abrupt decrease in brightness temperatures was detected at short wavelengths of $\lambda = (1.03, 1.38, 2.7)$ cm.

To compare the brightness temperatures found from observations of the eclipse on March 29, 2006 with brightness temperatures of the quiet Sun and large low-latitude CHs, the corresponding data were used, being taken in the years of the quiet Sun (1973–1976, 1984–1987) according to observations at close wavelengths with the Large Pulkovo Telescope and RATAN-600 (Borovik et al., 1990; Borovik, 1994). Figure 5 shows the brightness temperature distribution of the radio emission intensity at a wavelength of 6.2 cm found from observations of the solar eclipse and that of the radio emission intensity of the quiet Sun according to the data of Borovik et al. (1990) at a wavelength of 4.0 cm. The brightness temperatures determined from observational data of the solar eclipse at a wavelength of 6.2 cm are less than those at a wavelength of 4 cm for the quiet Sun; consequently, the polar CH of March 29, 2006 can be visualized at a wavelength of 6.2 cm.

Comparison of the brightness temperature distribution of the polar CH at a wavelength of 2.7 cm with that of the quiet Sun at a wavelength of 2.7 cm testifies to a full coincidence of brightness temperatures (Fig. 6). This is confirmed by the fact that the polar CH is not seen at a wavelength of 2.7 cm (Golubchina, 2021).

The low-latitude CHs can exist on the background of the quiet Sun in the years of the solar activity minimum. In this case, the open magnetic field lines produce a CH either as a result of the convective motions in the photosphere or by a reconnection of force lines of the open magnetic field with

Table 2. Brightness temperatures (Tb, K) of the quiet Sun (S1), mean semi-empirically coordinated model data of the low-latitude CH (CH1) on the background of the quiet Sun and polar CH (CH2) at close wavelengths. Here $\lambda^{(1)}$ denotes the data of Borovik et al. (1990); $\lambda^{(2)}$ – results of the observation of the eclipse on March 29, 2006 with RATAN-600, r/Rs is the normalized distance from the center of the solar disk to the points of the measurement, which are the closest to the solar limb during the solar eclipse.

$\lambda^{(1)}$ (cm):	6	15	31.6
(CH1); Tb, 10^3 K:	19.6	39	86
(S1); Tb, 10^3 K:	24.7	63	174
$\lambda^{(2)}$ (cm):	6.2	13	30.7
(CH2); Tb, 10^3 K:	14	45	84
r/Rs:	1.017	1.005	1.01

closed force lines (Fisk, Schwadron, 2001; Abramenko et al., 2006). In order to ascertain whether a dependence of the thermodynamical parameters of the CH plasma in the period of minimal solar activity on their localization on the Sun can exist, we have performed a comparative analysis. Table 2 lists the brightness temperatures of the radio emission of the quiet Sun, mean brightness temperatures of large low-latitude CHs according to the data of observations in the periods of the quiet Sun (Borovik et al., 1990), and brightness temperatures of the polar CH (29.03.2006) at close wavelengths of the centimeter range. The brightness temperatures of low-latitude CHs (CH1) on the background of the quiet Sun and brightness temperatures of the polar CH (CH2) at wavelengths $\lambda > 5$ cm are less than the brightness temperatures of the

quiet Sun (S1). This comparison indicates the practically equal in magnitude brightness temperatures of low-latitude CHs and the polar CH in points located near the solar limb at close wavelengths. This means that the properties of CHs do not depend on their location on the Sun, consequently, on the mechanism of generating CHs in the period of minimal solar activity (Golubchina, 2017).

4 Discussion

The analysis of observations of the solar eclipse on March 29, 2006 at the north-east sector of RATAN-600 was performed using the observational and theoretical data published by different authors. Numerous papers associated with studying the microwave radiation of CHs on the Sun note that the CHs at short wavelengths of the centimeter range cannot be seen. A possible reason of this phenomenon as well as the problem of the enhanced microwave radio emission of polar CHs on the Sun were studied by many researchers.

Observations of polar CHs were first carried out at CrAO at wavelengths of 8.2 and 13.5 mm (1974–1977) with the RT-22 radio telescope and the Culgoora Radioheliograph (Australia) at a wavelength of 3.5 mm with a 4 m paraboloid (Babin et al., 1976; Efanov et al., 1980). The CrAO observations of polar CHs were conducted at latitudes up to 80°. Observations in the radio range at larger latitudes are impossible due to a large gradient of the temperature near the solar limb. Polar CHs were detected to be the regions of enhanced radio emission intensity in the millimeter wavelength range. Thus, at $\lambda = 8.2$ mm an excess over the level of the quiet Sun is $dT = 1500$ K, whereas at $\lambda = 13.5$ mm – $dT = 2200$ K. The values of dT = 240–560 K were obtained according to the analogous measurements performed in Japan with the 45 m telescope at $\lambda = 8.3$ mm. Meanwhile, at a wavelength of $\lambda = 3.1$ mm no enhancement in intensity over the level of the quiet Sun was detected (Shimabukuro et al., 1975).

Particular attention was paid to the association between the enhancing millimeter radiation of a polar CH and the enhancing unipolar magnetic field inside a CH (Kosugi et al., 1986). In this paper, the results of observations with the 45 m radio telescope Nobeyama at the wavelengths of 8.3 and 3.1 mm (1984) show a brightening of (3–7) % at $\lambda = 8.3$ mm near the poles at the latitudes of $> 65°$. Searching for a reason of the enhanced radio emission intensity of a polar CH at short wavelengths, Gopalswamy et al. (1999) made use of the observations of solar radio emission at $\lambda = 1.76$ cm derived with the Nobeyama radio heliograph and the data of the extreme ultraviolet radiation (EUV) from the Solar Heliospheric Observatory (SOHO). The authors concluded that the radio enhancement was due to the "enhanced one-polar magnetic regions lying at the base of a coronal hole"; the structure of microwave brightening is composed of the smoothed and compact components. The point sources are associated with an interaction of elements of different polarity. To elucidate the enhancement in radio emission at 17 GHz near the solar poles, Selhorst et al. (2005, 2010) considered different models taking into account the randomly located solar spicules as well as spicules and small regions without spicules (interspicule holes), which in the maps of observations at 17 GHz are seen as bright spots in the pole region. The authors detected that the enhanced radio emission at $\lambda = 1.76$ cm is inhomogeneous with respect to the bright spots near the limb. Interspicule holes are located above the polar faculae, whereas the bright polar spots observed at $\lambda = 1.76$ cm are located close to the regions of polar faculae. These models are in good agreement with the results of observations of polar brightenings at $\lambda = 1.76$ cm. According to the observations at the Metsahovi Radio Observatory (Finland) and at $\lambda = (8, 3.4, 3.5)$ mm, white-light observations (Kislovodsk) as well as observations in ultraviolet (EUV SOHO) and soft X-rays (0.25–4 keV) the authors concluded that the enhancement in radio emission intensity of polar CHs can be associated with the appearance of polar faculae, plumes, bright points, and strong magnetic fluxes (Pohjolainen, 2000; Riehokainen et al., 2001). The brightening in CHs is sometimes unexplainable. Shibasaki (2013) assumed that the brightening of polar CHs can be caused by the effect of the heated atmosphere which outflows along the unipolar magnetic field of the open structure. Pasachoff (2007) note an observation of the bright plume during the solar eclipse on March 29, 2006. On the basis of the results of the listed papers one can assume that the higher brightness temperatures of the polar CH at the wavelengths of (1.03, 1.38, 2.7) cm and, hence, the absence of visibility of the CH at these wavelengths can be caused by the presence of polar faculae, plumes, and unipolar magnetic fields near the north pole of the Sun. The analysis of the obtained brightness temperature distribution of the polar CH was performed using the results of earlier observations of large low-latitude coronal holes and the quiet Sun with the Large Pulkovo Radio Telescope and RATAN-600 in the standard observation mode in years of the quiet Sun (Golubchina, 2021). The results of comparisons confirmed the actual registration of the coronal hole above the north pole of the Sun on March 29, 2006 at the wavelengths of (6.2, 13.0, 30.7) cm and the absence of CH visibility at the wavelengths of (1.03, 1.38, 2.7) cm. The identity of characteristics of equatorial and polar CHs was studied using the data on white-light observations of the CH with the coronagraph of the Skylab satellite (Munro, Jackson, 1977). The authors concluded that the "physical conditions inside the coronal hole do not depend on the individual localization on the Sun". The results of observations of the full solar eclipse on March 29, 2006 with RATAN-600 in the centimeter wavelength range confirmed this conclusion (Golubchina, 2021).

5 Conclusions

1. The observation of the solar eclipse on March 29, 2006 with RATAN-600 made it possible **for the first time** to determine the brightness temperature distribution above the north pole of the Sun within the limits of the polar CH on the Sun in a wide centimeter wavelength range of $\lambda = (1.03, 1.38, 2.7, 6.2, 13.0, 30.7)$ cm at a distance interval of (1.005–2.0) Rs from the center of the solar optical disk.
2. A dramatic increase in the brightness temperature of the radio emission from the polar CH at the centimeter wavelengths of $\lambda \geqslant 6$ cm near the solar limb, which confirmed the actual registration of the polar CH above the north pole of the Sun.

3. The polar CH is not seen at the short centimeter wavelengths of $\lambda = (1.03, 1.38, 2.7)$ cm.
4. The coincidence of brightness temperatures of the polar CH and large low-latitude CHs at close wavelengths in the northern hemisphere of the Sun is indicative of the identity of temperature properties of the polar CH and low-latitude CHs, regardless of their location on the Sun and, consequently, the mechanism of their formation in the period of the solar activity minimum.

References

Abramenko V.I., Fisk L.A, Yurchyshyn V.B., 2006. Astrophys. J., vol. 641, no. 1, pp. L65–L68.

Babin A.N., Gopasiuk S., Efanov V.A., et al., 1976. Izv. Krymsk. Astrofiz. Observ., vol. 55, pp. 3–13. (In Russ.)

Borovik V.N., Kurbanov M.S., Livshits M.A., et al., 1990. Sov. Astron., vol. 34, no. 5, pp. 522–530.

Borovik V.N., 1994. In Belvedere G., Rodono M., Simnett G.M. (Eds), Advances in Solar Physics. Lecture Notes in Physics, Berlin, Heidelberg: Springer, vol. 432, pp. 185–190.

Efanov V.A., Moiseev I.G., Nesterov N.S., et al., 1980. In Kundu M.R. and Gergely T.E. (Eds), Radio Physics of the Sun, Proceedings of the Symposium. Dordrecht: D. Reidel Publishing Co., vol. 86, pp. 141–144.

Fisk L.A., Schwadron N.A., 2001. Astrophys. J., vol. 560, no. 1, pp. 425–438.

Golubchina O.A., Korzhavin A.N., Tokhchukova S., 2011. Astrophys. Bull., vol. 66, no. 4, pp. 488–495.

Golubchina O.A., 2017. Geomagnetism and Aeronomy, vol. 57, no. 8, pp. 964–967.

Golubchina O.A., 2021. Astron. Rep., vol. 65, no. 4, pp. 322–330.

Gopalswamy N., Shibasaki K., Thompson B.J., DeForest C., and 2 more, 1999. Geophysical Research, vol. 104, no. A5, pp. 9767–9779.

Kosugi T., Ishiguro M., Shibasaki K., 1986. Publ. Astron. Soc. Japan., vol. 38, no. 1, pp. 1–11.

Munro R.H., Jackson B.V., 1977. Astrophys. J., vol. 213, no. 1, pp. 874–886.

Pasachoff J.M., Rušin V., Druckmüller M., et al., 2007. Astrophys. J., vol. 665, no. 1, pp. 824–829.

Pohjolainen S., 2000. Astron. Astrophys., vol. 361, pp. 349–358.

Riehokainen A., Urpo S., Valtaoja E., et al., 2001. Astron. Astrophys., vol. 366, no. 1, pp. 676–685.

Selhorst C.L., Silva A.V.R., Costa J.E.R., 2005. Astron. Astrophys., vol. 440, no. 1, pp. 367–371.

Selhorst C.L., Giménez de Castro C.G., Varela Saraiva A.C., et al., 2010. Astron. Astrophys., vol. 509. p. A51.

Shibasaki K., 2013. Publ. Astron. Soc. Japan, vol. 65, no. 1, p. S17.

Shimabukuro F.L., Wilson W.J., Mori T.T., et al., 1975. Solar Phys., vol. 40, no. 2, pp. 359–370.

Sobolev V.V., 1967. Kurs teoreticheskoi astrofiziki. M.: Nauka. (In Russ.)

Zheleznyakov V.V., 1964. Radioizluchenie Solntsa i planet. M.: Nauka. (In Russ.)